2013 MRS SPRING MEETING & EXHIBIT

Heat Transfer between a Hot AFM Tip and a Cold Sample: Impact of the air pressure

Journal:	*2013 MRS Spring Meeting*
Manuscript ID:	Draft
Manuscript Type:	Symposium V
Date Submitted by the Author:	n/a
Keywords:	calorimetry, differential thermal analysis (DTA), thermal conductivity

Complete List of Authors:
Chapuis, Pierre-Olivier; CNRS - INSA Lyon, CETHIL
Rousseau, Emmanuel; CNRS - Univ. Montpellier 2,
ASSY, Ali; CETHIL- INSA de Lyon,
Lefevre, Stephane; CETHIL- INSA de Lyon,
Gomes, Severine; CNRS - INSA Lyon, CETHIL
Volz, Sebastian; CNRS - Ecole Centrale Paris, Lab. EM2C

Heat transfer between a hot AFM tip and a cold sample: impact of the air pressure

Pierre-Olivier Chapuis[1,2], Emmanuel Rousseau[1,3], Ali Assy[2], Séverine Gomès[2], Stéphane Lefèvre[2], and Sebastian Volz[1]
[1]Laboratoire EM2C, Ecole Centrale Paris-CNRS, Grande voie des vignes, 92295 Chatenay-Malabry, France
[2]Centre de Thermique de Lyon (CETHIL), CNRS-INSA de Lyon-UCBL, 9 rue de la Physique, Campus La Doua-LyonTech, 69621 Villeurbanne (Lyon), France
[3]Groupe d'Etude des Semiconducteurs - CC074, Université de Montpellier II, Place Eugène Bataillon, 34095 Montpellier, France

ABSTRACT

We observe the heat flux exchanged by the hot tip of a scanning thermal microscope, which is an instrument based on the atomic force microscope. We first vary the pressure in order to analyze the impact on the hot tip temperature. Then the distance between the tip and a cold sample is varied down to few nanometers, in order to reach the ballistic regime. We observe the cooling of the tip due to the tip-sample heat flux and compare it to the current models in the literature.

INTRODUCTION

At nanometer scale probing the temperature [1] or measuring thermal properties such as the thermal conductivity [2] is a difficult task that may be tackled with scanning thermal microscopy (SThM) [3-4]. This technique is based on an atomic force microscope (AFM) with a tip sensitive to heat fluxes and/or temperature variations. SThM has been proposed for data storage [5–7], nano-lithography [8–10] or chemical sensing [11]. A key issue in local thermal analysis is to know the thermal sensitivity and the ultimate spatial resolution of the apparatus [12–14]. The resolution depends on the relative intensities of the heat fluxes transferred from the tip to the sample by various channels: conduction at their solid-solid contact; conduction in the liquid meniscus due to ambient humidity and located around the mechanical contact; air conduction around the tip [14]. The spatial resolution is linked to the contact area and improves when conduction though air and the water meniscus are removed. Working in vacuum (pressure lower than 10^{-2} mbar) removes the contribution from the surrounding air and might affect the water meniscus. It improves spatial resolution [15-16] but decreases the thermal sensitivity. An intermediate vacuum can be a compromise between spatial resolution and thermal properties sensitivity. In this study we focus on the heat flux due to conduction in air. We analyze the tip losses to the ambient environment and observe the cooling of the tip when approaching it close to the surface.

EXPERIMENTAL SETUP

We now turn to the description of the first experiment. Our setup consists in a SThM embedded in a vacuum chamber. The probe is a 75 μm diameter Wollaston wire which is etched at its ends on approximately 200 μm. The outer part (silver) has been removed so that the inner

Pt90/Rh10 part of diameter 5 µm is apparent and bent in a V shape at its extremity. This probe has been extensively described in the past [17-18]: An electrical current heats the etched part of the wire though Joule effect. The probe can be heated alternatively by a DC or an AC current [18] and acts in the same time as the heater and the temperature sensor. When the average temperature of the probe varies a change in the probe electric resistance is induced, which leads to a modification of its voltage. Thus we are able to monitor the tip average temperature variations by monitoring the probe voltage. We use a Wheatstone bridge balanced at low current (no heating: Tip at room temperature) to observe a voltage signal directly proportional to the increase of temperature. When the tip is in contact with a sample, the probe cools down because heat is flowing through this contact. This allows observing thermal properties of samples.

RESULTS

Heat losses in the ambient air

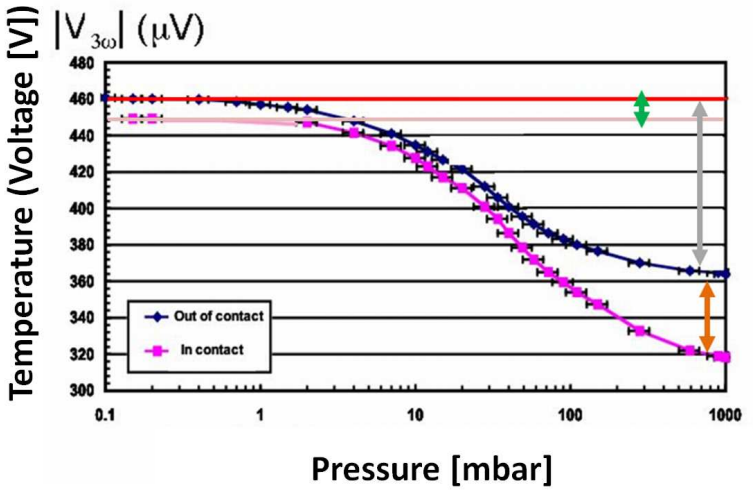

Figure 1. Tip voltage $V_{3\omega}$ as a function of the chamber pressure (low vacuum) in the AC mode (I_0 = 30 mA and f=70 Hz). (a) Pink line: Tip/sample contact (b) Blue line: Tip removed far away from the sample.

From ambient, the pressure in the vacuum chamber is varied down to approximately 0.1 mbar. Figure 2 shows the third-harmonic tip voltage as a function of the pressure, for two cases: (a) Tip and sample in contact and (b) tip removed far away from the sample (~3 mm). In this so-called 3ω mode [14], the tip's third harmonic voltage $V_{3\omega}$ is proportional to the second harmonic of the temperature $\theta_{2\omega}$: $V_{3\omega} = RI_0/2\ \theta_{2\omega}$, where R is the tip's electrical resistance, I_0 the input current's intensity, $\alpha = d\rho_e/dT$ and ρ_e is the Pt90/Rh10 resistivity. At sufficiently low frequency, the temperature field out of the tip is supposed to be in the stationary regime. Arrows underline the temperature differences between the (a) and (b) cases at ambient pressure (orange), between (a) and (b) at low pressure (< 0.1 mbar, green) or between (b) at ambient and (b) at low pressure (grey). At low pressure, the temperature reaches a plateau: it appears that the heat flux does not depend anymore on the pressure. First, we observe that removing the air losses increases the temperature by about 30 % when the probe is in contact and 20 % when out of contact. Second, the heat losses in the air are 2.5 times larger than the one to the sample (grey vs. orange arrows). Finally, the heat flux flowing into the sample is three times more important at ambient pressure

than at low pressure (green vs. orange arrows). As a consequence, the heat transfer through the air is the most important channel to lose heat for this kind of tip. This is due in particular to the large size of the tip [14].

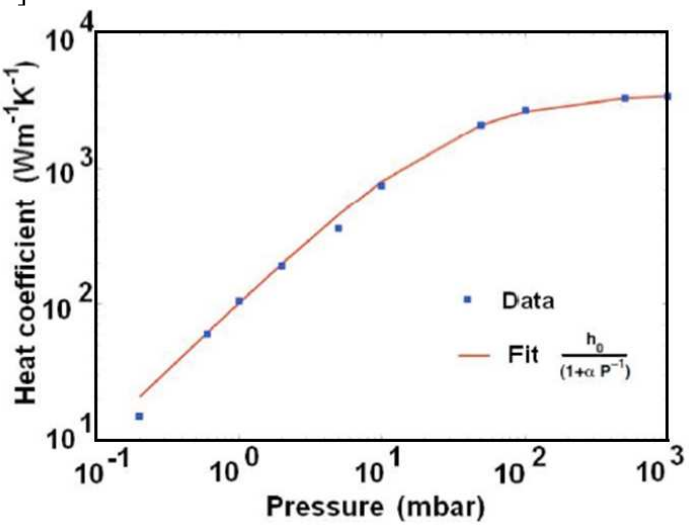

Figure 2. Mean heat transfer coefficient (AC mode) vs. pressure. The behavior is linear at low pressures, due to ballistic heat transfer.

The comparison of the experimental values with a model of the temperature in the tip [14, 19] enables to estimate the heat losses from the tip in the air (blue curve). These losses are taken into account by an effective heat transfer coefficient h at the fin's walls. This coefficient accounts for heat conduction and convection in air. We find $h(P)$ by comparing our model with the measurements (see Fig. 2). The value at the ambient pressure is relatively high $h(1\text{bar}) \sim 5000$ $\text{Wm}^{-2}\text{K}^{-1}$ as it should be when characteristic sizes are smaller than the convective boundary layer. At low pressures $h(P)$ shows a linear dependence. This is due to the ballistic heat transfer between the tip and the apparent walls of our geometry [20] (walls of the microscope, of the sample, of the vacuum chamber). Indeed the mean free path Λ of air molecules, which is inversely proportional to the pressure [20], takes values on the order of millimeters at $P = 10^{-1}$ mbar. We compare our experimental data with a model developed by Lees and Liu [20]. They have calculated the heat transfer between two concentric cylinders (radii $R_2 > R_1$) by taking into account the transition between the diffusive and ballistic regimes. They found the following relation for the heat flux:

$$\phi = \frac{\phi_F}{1 + 1 \Big/ \left(1 + \frac{4}{15} Kn_1^{-1} + \ln \frac{R_2}{R_1} \right)}, \qquad (1)$$

where ϕ_F is the corresponding fully diffusive flux and $Kn_1 = \Lambda_1/R_1$ is the Knudsen number associated with cylinder 1 (taken at T_1). $\Lambda_1 = (\mu_1/2\rho_1)\, 2\pi m\, k_B T_1$ is the related mean free path, with μ being the dynamic viscosity, ρ the density, m the molecule mass and k_B the Boltzmann constant. Only the density depends on the pressure and we assume that it is inversely proportional. A fit of the data in Figure 2 shows a good agreement between the model by Lees

and Liu and the experiment. The transition from diffusive to non-Fourier regimes occurs for a pressure close to P~10 mbar. From the fit parameter, assuming a dynamic viscosity equal to μ = 18 Pa.s, we find an equivalent outer radius of R_2 = 10 microns, smaller than the distance to the closer object (microscope head) in the chamber but of the same order of magnitude than the convective boundary layer. Since natural convection is not taken into account in the model by Lees and Liu, this model with reduced outer radius enables to bridge pure conduction in the boundary layer and natural convection.

Heat transfer between the tip and a substrate

We now describe our second experiment where the tip voltage is measured as a function of the tip-sample distance d. The tip is heated with a DC current in order to prevent from intermittent contact due to harmonic dilatation of the wire in AC heating. The tip voltage is again proportional to the average probe temperature ($V=\alpha R I_0 \theta$) where θ is the tip average temperature variation.

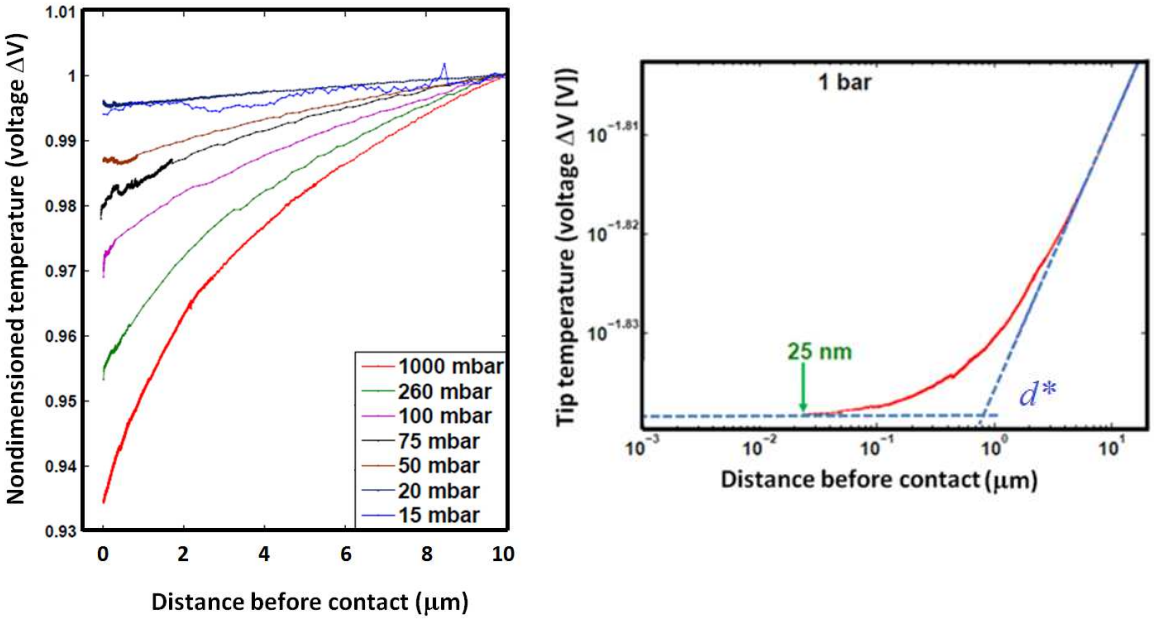

Figure 3. Temperature estimated from the tip voltage (DC mode) vs. distance. a) Normalized temperature as a function of various pressures for the last 10 microns before contact. b) Results at ambient pressure (log. scale).

Figure 3a shows the tip voltage divided by its value for d=10 μm in the last 10 μm before contact. The distance is measured with the AFM piezo-actuator signal and the contact point is detected thanks to the large deflection of the AFM photodiode when reaching the contact. Note that the absolute distance is plotted here, since the tip attraction by the sample due to various interaction forces has been compensated by monitoring the evolution of the deflection signal out of contact. Before the contact, we observe a steeper slope in the voltage-distance curve meaning that there is a significant tip-sample thermal exchange. Around 6.5% of the temperature is 'lost'

at ambient pressure in the last 10 microns. In contrast, when the pressure is lowered, the temperature is maintained within a percent for pressures of a few dozens of millibars.

We observe in Figure 3b the well-known jump that occurs just before contact due to the interaction forces. As a consequence, a domain of distances of 25 nm is not available here. However, a large range of distances can be plotted and the distance scale is logarithmic. The temperature drops linearly for distances larger than 5 μm as shown by the superimposed dashed blue line. The tip temperature appears to level off for distances on the order of 25 nm. The plateau (horizontal dashed line) intercepts the extension of the Fourier regime (dashed blue line) for a characteristic distance d^* ~800 nm.

DISCUSSION

In order to understand this behavior we compare our experimental data with calculations done for a vertical half torus of radius of curvature R_c=15 μm kept at constant temperature, a geometry which is similar to the hot extremity of the tip (not shown here. See [27]). We first verify that heat flux lines can be supposed vertical and the temperature constant in a section of the torus for sufficiently-small values of d. By considering that a tip elementary surface element exchanges a flux $\delta\phi=\delta G \Delta T$ with its projection on the sample δS, with

$$\delta G = \frac{\lambda_0}{d + C\Lambda}\delta S \ , \qquad (2)$$

we observe that a curve with a similar shape to Figure 3b can be reproduced. However, for C~1, the characteristic distance d^* is then much smaller than the experimental one, on the order of few tens of nanometers ($d^*_{simulated}$~ 20 nm for a mean free path Λ on the order of 60 nm). Note that in Eq. 2 λ_0 is the air thermal conductivity at room temperature. Such an expression allows to retrieve the diffusive flux when d is large (i.e. $\delta G = \lambda_0/d$) and a constant conductance when two surfaces are very close, which is typical for the ballistic thermal conduction. It appears that this approach is not sufficient. The roughness of the tip should also be taken into account, as it is of the same order of magnitude than the air molecule mean free path.

CONCLUSIONS

In conclusion, we have characterized a hot micrometric tip which is used for local thermal analysis. We have shown that a very significant part of the heat transfer between the tip and a sample is due to air heat conduction. Vacuum may be considered as an ideal environment for the use of the SThM, but one should then account for heat exchanges which are very different from the ones at ambient pressure.

ACKNOWLEDGMENTS

We acknowledge the supports of ANR through the *Monaco* project and of *Fédération Francilienne de Transferts de Masse et de Chaleur*. We thank the members of CNRS research networks ”Micro et Nanothermique” and ”*Thermique des nanosystèmes et nanomatériaux*” for discussions. We warmly thank J.J Greffet for his help and S.K. Saha for his stay.

REFERENCES

1. C.C. Williams and H.K. Wickramasinghe, *Appl. Phys. Lett*. 49, (1986), 1587
2. G. B. M. Fiege, A. Altes, R. Heiderhoff and L. J. Balk, *J. Phys. D: Appl. Phys*. 32 , L13 (1999).
3. R.B. Dinwiddie, R.J. Pylkki and P.E. West, Thermal conductivity contrast imaging with a scanning thermal microscope, *Thermal conductivity* 22, T.W. Wong ed, Tecnomics, Lancaster PA, 668-677, 1994
4. A. Hammiche, H.M. Pollock, M. Song, D.J. Hourston, *Rev. Sci. Instrum*. 67, 4268 (1996)
5. P. Vettiger, G. Cross, M. Despont, U. Drechsler, U. Dürig, B. Gotsmann, W. Häberle, M.A. Lantz, H.E. Rothuizen, R. Stutz and G. K. Binnig, *IEEE Trans. on Nanotech*. 1, 39 (2002)
6. W.P. King and K.E. Goodson, ASME *J. Heat Transf*. 124, 597, (2002)
7. W. A. Challener et al. *Nature Photonics* 3,220 (2009).
8. A. Chimmalgi, D.J. Hwang, and C.P. Grigoropoulos, *Nano Lett*. 5, 1924 (2005)
9. A.A. Milner, K. Zhang, and Y. Prior, *Nano Lett*. (2008)
10. O. Fenwick, L. Bozec, D. Credgington, A. Hammiche, G. M. Lazzerini, Y. R. Silberberg and F. Cacialli, *Nature Nanotechnology* 4, 668 (2009)
11. R. Szoszkiewicz, T. Okada, S. C. Jones, T.-D. Li, W. P. King, S. R. Marder, and E. Riedo, *Nano Lett.* 7, 1064 (2007)
12. P.O. Chapuis, J-J. Greffet, K. Joulain and S. Volz. *Nanotechnology* 17, 2978 (2006).
13. Microscale and Nanoscale Heat Transfer, *Topics in Applied Physics* 16, Vol. 107, S. Volz d., 2007
14. S. Lefèvre, S. Volz and P.-O. Chapuis. *Int. J. Heat Mass Transf*. 49, 251 (2006).
15. L. Shi and A. Majumdar, *ASME J. Heat Transf*. 124, 329 (2002)
16. M. Hinz, O. Marti, B. Botsmann, M.A. Lantz and U. Dürig. *Appl. Phy. Lett*. 92, 043122 (2008).
17. S. Lefèvre, S. Volz, C. Fuentes, J.B. Saulnier and N. Trannoy, *Rev. Scient. Instr*. 74, 2418 (2003)
18. S. Lefèvre and S. Volz, *Rev. Scient. Instr*. 76, 033701 (2005)
19. P.-O. Chapuis, *PhD Thesis*, Ecole Centrale Paris (2007)
20. L. Lees and C.Y. Liu, Phys. of Fluids 5, 1137 (1962)